UC Irvine
UC Irvine Previously Published Works

Title

Constraining ice dynamics at Dome C, Antarctica, using remotely sensed measurements

Permalink

Journal

ISSN

Authors

Legresy, Benoit
Rignot, Eric
Tabacco, Ignazio E

Publication Date

DOI

Copyright Information

Peer reviewed

Constraining Ice Dynamics at Dome C, Antarctica, Using Remotely Sensed Measurements

Benoit LEGRESY,

LEGOS (CNRS-CNES-UPS) Toulouse, FRANCE, e-mail: benoit.legresy@cnes.fr

Eric RIGNOT,

JPL (NASA) Pasadena, CA USA, e-mail: eric@adelie.jpl.nasa.gov

and Ignazio E. TABACCO,

DST-Geophysica, Milano, ITALY, e-mail: tabacco@imiucca.csi.unimi.it

Abstract. A first time description is given of the ice flow at Dome C, Antarctica, around the EPICA drilling site. We used satellite radar altimetry to obtain the precise ice surface topography, airborne radio echo sounding to obtain the ice thickness and satellite SAR interferometry to derive one component of the surface velocity field. The balance flux around the Dome C area is then accurately mapped and comparisons made between driving stress, surface and balance velocity to help us describe the ice flow in the region. As a by-product of the study, we also recover anomalies in the ice flow conditions in sub-glacial lake locations. These effects result from localy invalid shallow-ice approximation. The results of this study form the basis for future investigations of the ice flow conditions at Dome C in relation to ice core interpretation.

Introduction

The EPICA (European Project on Ice Core drilling in Antarctica) chose Dome C as the site to perform the deepest drilling in Antarctica. The choice of this site was guided by the fact that around the summit of Dome C, the horizontal movement of the ice surface is negligible and thus the total ice column is formed by snowfall accumulation. Hence analysis of the ice cores gives a direct measure of the climate evolution at this place. The aim of this paper is to demonstrate how the use of remotely sensed data can help understand the ice movement around the EPICA drilling site. We map the balance, deformation and surface velocities using surface topography, thickness and interferometric synthetic aperture radar data. Finally, we compare all of these velocity fields and draw some conclusions about the ice movement around Dome C.

Datasets. The ice surface topography has been computed using radar altimeter data from the ERS1 geodetic cycle during 1994-1995 [*Remy et al.*, 1999].

The chosen grid spacing is a compromise between the radar footprint (2-3 km diameter) and the along and cross track resolution. The mapped spatial resolution is thus 1/30 degree (i.e., 3.7 km in a north-south direction and 1 km in east-west direction). All calculations presented in this paper refer to this grid unless otherwise indicated. The height precision of the mapped topography has been evaluated by comparison with a kinematic GPS survey [*Ceffalo et al.*, 1996] and agreement is at an rms level of 20 cm. The ice thickness data are the result of an airborne radio echo sounding survey [*Tabacco et al.*, 1998] collected over a 80*120 km rectangular grid with a 10 km across track grid spacing, refined to 5 km in the central region. These data have been interpolated [*Remy and Tabacco*, 2000] to the same 1/30 degree grid as the ice surface topography and the difference gives the bedrock topography. Finally, two ERS SAR acquisitions have been used to perform the interferometry. The SAR scene selection was difficult as there was no data available from ascending tracks over Dome C and only a few useful scenes on the descending tracks. At Dome C, the ice flow is slow (0-20 cm/a) and thus it is necessary to use a long temporal baseline (typically of the order of 70 days or more) to resolve a significant signal. It is also important to keep any radar coherence between the two acquisitions to form the interferogram. The coherence between scenes decreases with time separation (the surface state changes) and with orbital separation between the 2 acquisitions (if the ground target is not seen with the same incidence angle, the target response will differ). It is therefore important to have short orthogonal baselines. Many attempts at forming interferograms with long baselines lead to incoherence and no result. We only found one image pair (descending pass), centered at Dome C, with a 45 m orthogonal baseline. These data were from orbits ERS1-24781 in April 1996 and ERS2-4106 (frame 5193) in February 1996, with the time separation being 69 days.

Velocity field construction.

Balance velocity. The balance velocity results from the equilibrium between the snow accumulated on the ice cap (vertical flux) and the ice flow (horizontal ice

flux). The ice cap is assumed stationary and the to-
tal ice column is assumed to flow in the same direction
(i.e., in the direction of greatest slope), in other words
the shallow ice approximation is used. The balance ve-
locity can thus be represented as the mean value of the
ice column horizontal velocity assuming a plane flow:

$$U_B(x) = \frac{1}{H} \int_{top}^{x} acc(x')dx' \qquad (1)$$

where H is the ice thickness, *acc* the accumulation rate
and x the abscissa along the flow line from the top of
the dome. The integration is performed along a flowline
following the greatest slope. We computed the balance
velocity on a 5 km grid using the method of *Budd and
Warner*, [1996]. We experimented with many horizon-
tal spatial scales to compute the slope, ranging from
10-30 km (3-10 times the ice thickness), but did not
find any major differences, perhaps because the slopes
were small. The value of 10 km (which corresponds to
the resolution of our basic datasets) gave a more de-
tailed resolution for the flow direction. Balance fluxes
($U_B * H$ in m/a) are computed over the whole domain
surrounding Dome C since they do not need the knowl-
edge of the ice thickness. The accumulation rate (0.04
m/a) is taken from *Petit et al.*, [1982], based on a nu-
clear analysis of snow pits. Since the correlation length
scale of various accumulation rate compilations is of the
order of 100 km, the assumption of constant accumula-
tion over our area of interest is reasonable. The balance
velocity (Figure 1) is then obtained by dividing by the
ice thickness and projected to a geographical grid. To
first order, the ice velocity field is a divergent flow, start-
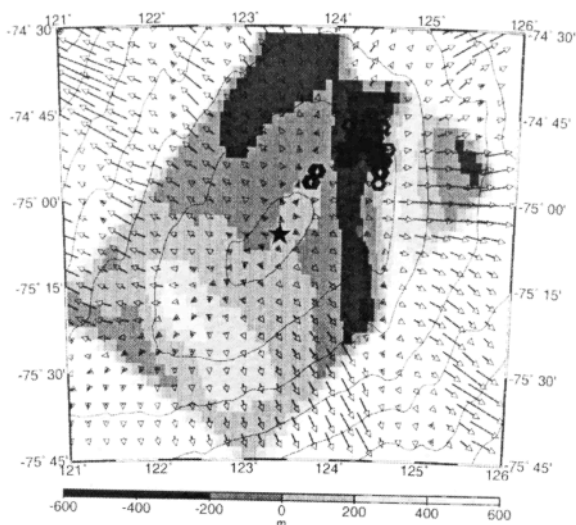ing from the top of the summit, with iso-values form-

Figure 1. Map of the ice balance flux (arrows) in the
Dome C area, the gray scale corresponds to the high
resolution bedrock topography, the isoline to the high
precision surface topography, the star to the EPICA
drilling site and circles to sliding areas detected by com-
paring InSAR surface velocities to driving stresses.

ing concentric ellipses. More rapid flow corresponds to
bedrock troughs, where the ice flow seems to converge.
For example, part of the west-east flux coming from
Dome C towards the mountain near 125E is redirected
northward and southward. The horizontal balance ve-
locity values range from 0 near the drilling site to 25-30
cm/a at 25 km from the summit or 3200 m elevation.

Driving stress. The driving stress (τ_d) is the main
force acting on the ice column and is responsible for the
ice deformation. We estimated τ_d components using the
precise ice topography (h), slope and thickness (H) as

$$\begin{cases} \tau_{dx} = \rho g H \frac{\partial h}{\partial x} \\ \tau_{dy} = \rho g H \frac{\partial h}{\partial y} \end{cases} \qquad (2)$$

where ρ is the density of ice, g the gravity constant,
x and y are horizontal coordinates. Here, longitudinal
stress is not accounted for since it is difficult to esti-
mate a-priori. But the high spatial resolution of the
dataset would help to decide whether this stress is sig-
nificant or not. Since there has not been significant ice
deformation at Dome C to give it a preferential orienta-
tion, horizontal isotropy is assumed. The deformation
velocity is defined as a function of the driving stress :

$$U_D = -HA\tau_d|\tau_d|^{(n-1)} \qquad (3)$$

where A and n are ice constitutive law parameters (see
[*Glen*, 1955; *Paterson*, 1994] for detailed description).
This deformation velocity only refers to local quantities
(thickness and slope) and is not a priori dependent on
the history of the flow from Dome C, in the same way as
the balance velocity is. Thus this calculation provides
an independent estimation of the way that the ice flows.

SAR Interferometry. We computed phase dif-
ferences between the two SAR acquisitions using both
NASA/JPL and CNES (DIAPASON) software. The co-
herence level between the images is of the order of 0.35.
The fringe pattern is based on [Rignot et al., 1995]:

$$\delta\phi = \frac{4\pi}{\lambda}(B\cos(\alpha + \theta) + \delta t V.r) + \phi_{orb} \qquad (4)$$

where λ is the radar wavelength (5.6 cm), B the or-
bital separation between the two data acquisitions, α
the baseline angle with respect to the horizontal, r the
unit range vector, θ the topography dependent angle
of r, δt the time separation between the two acquisi-
tions, V the surface velocity vector, ϕ_{orb} is the resid-
ual phase signal linked to any data uncertainties in the
area. The height of the phase ambiguity (topographic
change necessary to produce one fringe) is of the order
of 150 m and is computed at each point with the topo-
graphic correction applied using the surface elevation
data. The topographic correction is however less than
one fringe given the flatness of the area. The main sig-
nal present in the computed interferogram is composed
of a constant slope, which is also the case for the bal-
ance and deformation velocities projected in the SAR
line of sight. In such cases, it becomes difficult to sep-

arate between velocity-induced fringes and residual or-
bital fringes, which usually appear as linear ramps. We
computed the interferogram using both the ESA precise
orbits and Delft orbits data [*Scharoo and Visser,* 1998].
The first set of orbits introduced many fringes and we
separated the orbital fringes by least squares fitting of
the interferometric fringe pattern to a simulated fringe
pattern based on the balance velocities. The Delft or-
bits lead to the same result, but without the need for
any fitting. We therefore assumed that the Delft orbits
were precise enough and did not contain any residual
orbit signal. The final interferogram consisted of 2 1/2
fringes. The phase was further unwrapped using the
Goldstein et al., [1994] method. The error in the phase
estimation is expected to be very small, since the tropo-
sphere is particularly dry at Dome C. Since the fringe
pattern is simple, we estimated an error of 6 mm/a in
the velocity based on the above phase noise. However,
an absolute error from orbital uncertainties can still re-
main in the data at the same error level. We further
assume a total error of 1 cm/a for the data in the fol-
lowing section. The resulting SAR velocities represent
ice surface velocities, whilst the balance and deforma-
tion velocities refer to column-averaged velocities.

Comparison of the different velocity fields.
Having only one direction of SAR acquisition, we can-
not extend the SAR measurement into two directions.
We thus project all datasets in the horizontal plane and
in the SAR line of sight direction. Figure 2 shows the
maps of the projected driving stress, balance velocity
and SAR velocity. We computed correlation coefficients
to compare the different datasets. Comparing balance
and SAR velocity (Figure 3a) leads to a 0.82 correlation,
the scatter plot indicating a clear linear correspondence
between both velocity estimations. (Standard theory
for isothermal flow predicts a $(n+1)/(n+2)$ factor be-
tween both, but the noise level prevents any conclusion
between $n=1$, 2 or 3) A discrepancy arises, however,
for high velocities (>0.12 m/a), and we can see from
Figure 2 that this mostly comes from the fact that the
balance velocity is sensitive to the bedrock holes - see
for example, near location (74.75S, 122.5E) or in the
large valley near (124.5E). Adopting a vertical profile
of the horizontal velocity, with most of the variation
in deeper layers and a constant over the higher layers,
the ratio between surface and average velocity varies
inversely proportional to the ice thickness. This could
also be the result of the vertical profile to longitudinal
stresses present in the ice around bedrock depressions.
The comparison between tau_d and V_{SAR} is interesting
- see Figure 3b. The correlation coefficient is -0.83.
This relation between V_{SAR} (the surface velocity) and
τ_d is just an expression of the constitutive law of the ice
flow. One can observe a power relation between both
variables but it is difficult to compute a unique curve
fit using least squares estimation as the distribution of
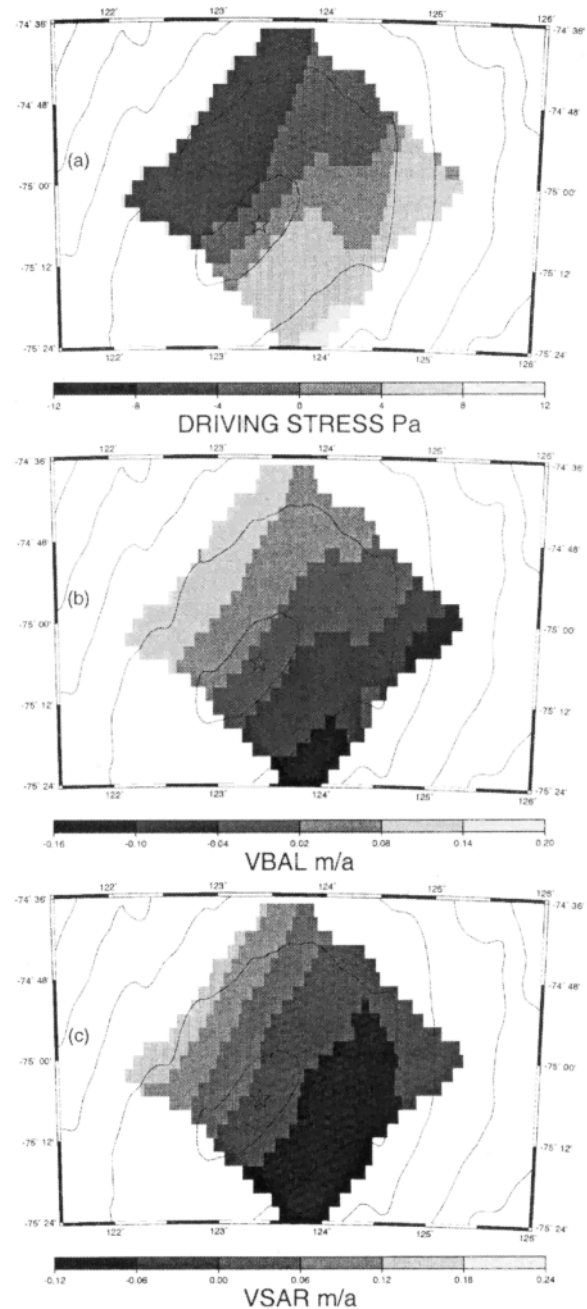data is too variable. A value for the Glen exponent

Figure 2. Maps of the computed flow parameters, pro-
jected in the SAR look direction : (a) the driving stress
in Pa, (b) the balance velocity in m/a and (c) the IN-
SAR surface velocity in m/a.

[*Glen,* 1955] of 2 or 3 provides a good fit to the data,
most of the misfit coming from our imprecise knowledge
of the absolute velocity field and the error level. The
values close to zero in Figure 3b correspond to (i) the
dome area and, (ii) areas where the driving stress and
velocity are mostly orthogonal to the line of sight. The
region of Figure 3b having the same sign for stress and
velocity (lower left, see box) is anomalous as the con-
stitutive law of ice flow requires opposite signs and so
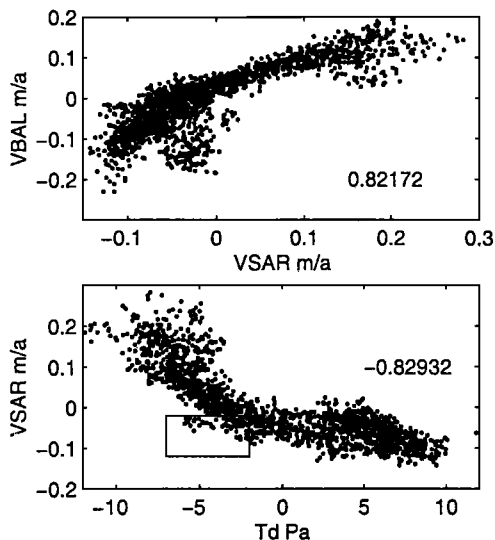these values are physically implausible. Regions where

Figure 3. Scatter diagrams of the three computed flow parameters : (a) the balance velocity against the surface velocity, (b) the surface velocity against the driving stress. Correlation coefficients are indicated within the diagram.

these anomalous values occur correspond to sliding areas. When sliding occurs on small size lakes, the lower part of the ice column is accelerated to ensure continuity, while the upper part of the ice column maintains a uniform velocity. A small anomaly (depending on the size of the lake) appears in the surface topography and hence in the driving stress. This mechanism can lead to very low stresses and surface velocities remaining of the same order of magnitude. Furthermore, sliding may locally change the direction of the ice flow. Hence, the projections of driving stress and surface velocity can have the same sign. In other terms, the shallow-ice approximation no longer holds. In any case, the areas corresponding to this kind of condition correspond to lakes detected by radio echo sounding, for example at (74.95S, 123.7E), the lake closest to Dome C and also at (74.9S 124.5E), a lake referenced by [*Siegert et al.*, 1996]. The areas showing these properties are displayed as circles on Figure 1. Finally the correlation between U_B and τ_d is-0.91.

Summary. In this paper, we investigated the flow of ice at Dome C in the area surrounding the deep drilling site. We demonstrated that remotely sensed data may help describe the ice flow by mapping a number of physical parameters of concern for ice flow studies. Ice surface velocities are well recovered from a 69 day temporal baseline ERS interferogram, the balance velocity is accurately mapped using surface and bedrock topographies and the driving stress can also be well described. We found that the shalow-ice approximation is not valid over small sub-glacial lakes. It appears that a method to recover sub-glacial lakes can be achieved using precise topography and velocity. However, our analyses lack an ascending ERS track for a full INSAR description of the surface velocity and of an absolute velocity reference. This situation can be overcome easily with future acquisitions of ERS2 or ENVISAT data. In

situ measurements of ice surface velocity will be beneficial to extend the analysis using in situ Doris and GPS surveys (C. Vincent and A. Cappra, personal comm.). The very slow movement (less than 1 cm/a) around the drilling site indicates that the ice present in the core may not have moved more than 1 km from that point, even for very old (deep) ice particles. *Van der Veen and Whillans,* [1992] showed that there can be discrepancy between the summit of the topography and the flow centre, but addressing this point will require additional and absolute measurements. Additionally, it would be of importance to have an improved measurement of this surface velocity and use modeling to constrain the flow divergence with depth, i.e., the longitudinal strain rate vertical profile [*Bolzan,* 1985].

References

Bolzan, J.F. Ice flow at the Dome C ice divide based on a deep temperature profile. J.Geophys. Res., 90D5, 8111-8124, 1985.

Budd W.F. and R.C. Warner. A computer scheme for rapid calculations of balance-flux distributions. Ann. Glaciol. 23, 21-27. 1996.

Ceffalo R., I.E. Tabacco and G. Manzoni. Processing of cinematic GPS trajectories at Dome C (Antarctica) and altimetry interpretations. Reports on survey and geodesy 25 pp. Bologna, Distart Ed Nautilus. 1996.

Glen, J.W. The creep of polycristalline ice. Proc. R. Soc. London A228, 519-538. 1955.

Goldstein, R.M., H.A. Zebker and C.L. Werner. Satellite Radar Interferometry : Two-dimensional Phase Unwrapping. Radio Science 23. 713-720. 1988.

Paterson W.S.B. The Physics of Glaciers. 3rd Ed. Pergammon Press Oxford. 1994.

Petit, J.R. J. Jouzel, M. Pourchet and L. Merlivat. A detailed study of snow accumulation and stable isotope content in the Dome C (Antarctica) area. J. Geophys. Res., 87(C6): 4301-4308. 1982.

Remy F., P. Schaeffer and B. Legresy. Ice flow physical processes derived from ERS1 High resol. map of Antarctica and Greenland Ice sheets. Geop. J. Int. 139, 645-656. 1999

Remy F. and I.E. Tabacco. Basal erosion network near the EPICA ice core site (Dome C, Antarctica). Geophys. Res. Lett., 27(3): 405-408. 2000.

Rignot, E., K.C. Jesek and H.G. Sohn.. Ice flow dynamics of the Greenland ice sheet from SAR Interferometry. Geophys. Res. Lett., 22(5): 575-578. 1995

Scharroo R. and P. Visser. Precise orbit determination and gravity field improvement for the ERS satellites, J. Geophys. Res., 103(C4): 8113-8127. 1998.

Siegert, M.J., J.A. Dowdeswell, M.R. Gorman and N.F. McIntyre. An inventory of Antarctic sub-glacial lakes. Antarct. Sci. 8(3): 281-286. 1996.

Tabacco, I.E., A. Passerini, F. Corbelli and M. Gorman. Determination of the surface and bed topography at Dome C East Antarctica. J. of Glaciol. 44, 185-191. 1998.

Van der Veen C.J. and I.M. Whillans. Determination of a flow center on an ice cap. J. of Glaciol. 130: 412-416. 1992.

B. Legresy, LEGOS, 18 Av. E. Belin , 31401 Toulouse cedex 4 FRANCE.